Aaltonen et al., http://www.jcb.org/cgi/content/full/jcb.201602007/DC1

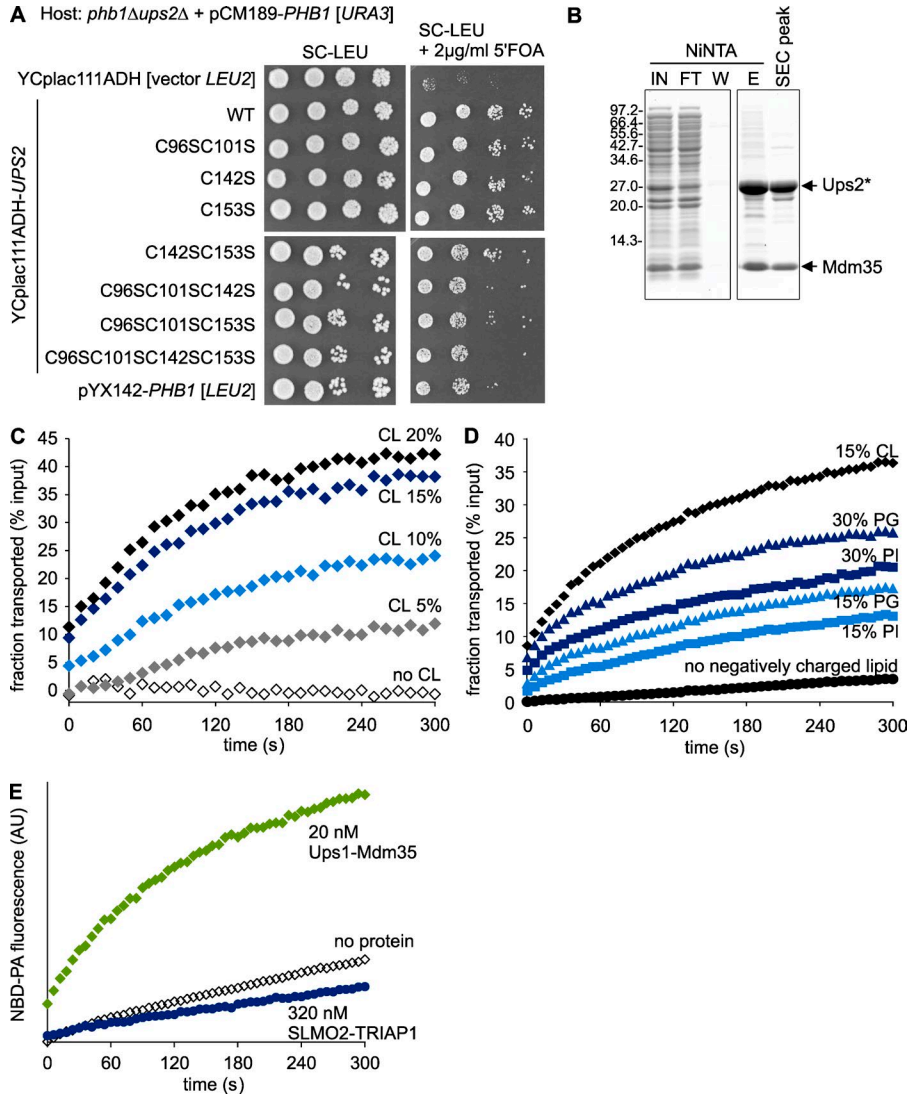

Figure S1. **Functionality in vivo and lipid transfer activities in vitro of lipid transfer protein complexes, related to Fig. 1.** (A) Ups2 mutants lacking cysteine residues are functional in vivo. Serial dilutions of Δ*phb1*Δ*ups2* (*PHB1*) cells expressing C-terminally myc-tagged Ups2 or its mutant variants harboring the indicated amino acid exchanges were spotted on media with or without 5-fluoroorotic acid (5′FOA), which counterselects against cells harboring the Phb1 expression plasmid. For control, cells carrying *LEU2* plasmid with an additional copy of *PHB1* were spotted. (B) Purification of hexahistidine-tagged Ups2$^{C96S/C101S/C142S/C153S}$ (Ups2*)–Mdm35. Lysates from *E. coli* cells overexpressing Ups2* and Mdm35 (IN), the flow-through (FT), wash (W), and elution (E) fractions of Ni-NTA affinity chromatography, and the peak fraction of the subsequent size exclusion chromatography (SEC, superdex75pg) were analyzed by SDS-PAGE followed by staining with Coomassie brilliant blue. (C) CL-dependent NBD-PS transfer by Ups2*–Mdm35. Ups2*–Mdm35 (160 nM) was incubated with donor liposomes (12.5 μM, containing 5% NBD-PS, 2% Rhodamine-PE, and tetraoleoyl-CL at the indicated concentrations) and acceptor liposomes (50 μM, containing tetraoleoyl-CL at the indicated concentration but no NBD-PS or Rhodamine-PE). NBD fluorescence was recorded. Maximum fluorescence in the absence of quenching was set to 100%. Spontaneous transport in the absence of protein was subtracted. (D) PI and PG facilitates NBD-PS transfer by Ups2*–Mdm35. NBD-PS transfer was assessed as in C in the presence of PI or PG at indicated concentrations in both donor and acceptor liposomes. (E) SLMO2–TRIAP1 did not facilitate intermembrane transfer of NBD-PA. Transfer of NBD-PA by SLMO2–TRIAP1 (at the indicated concentrations) was monitored. Ups1–Mdm35 served as a positive control.

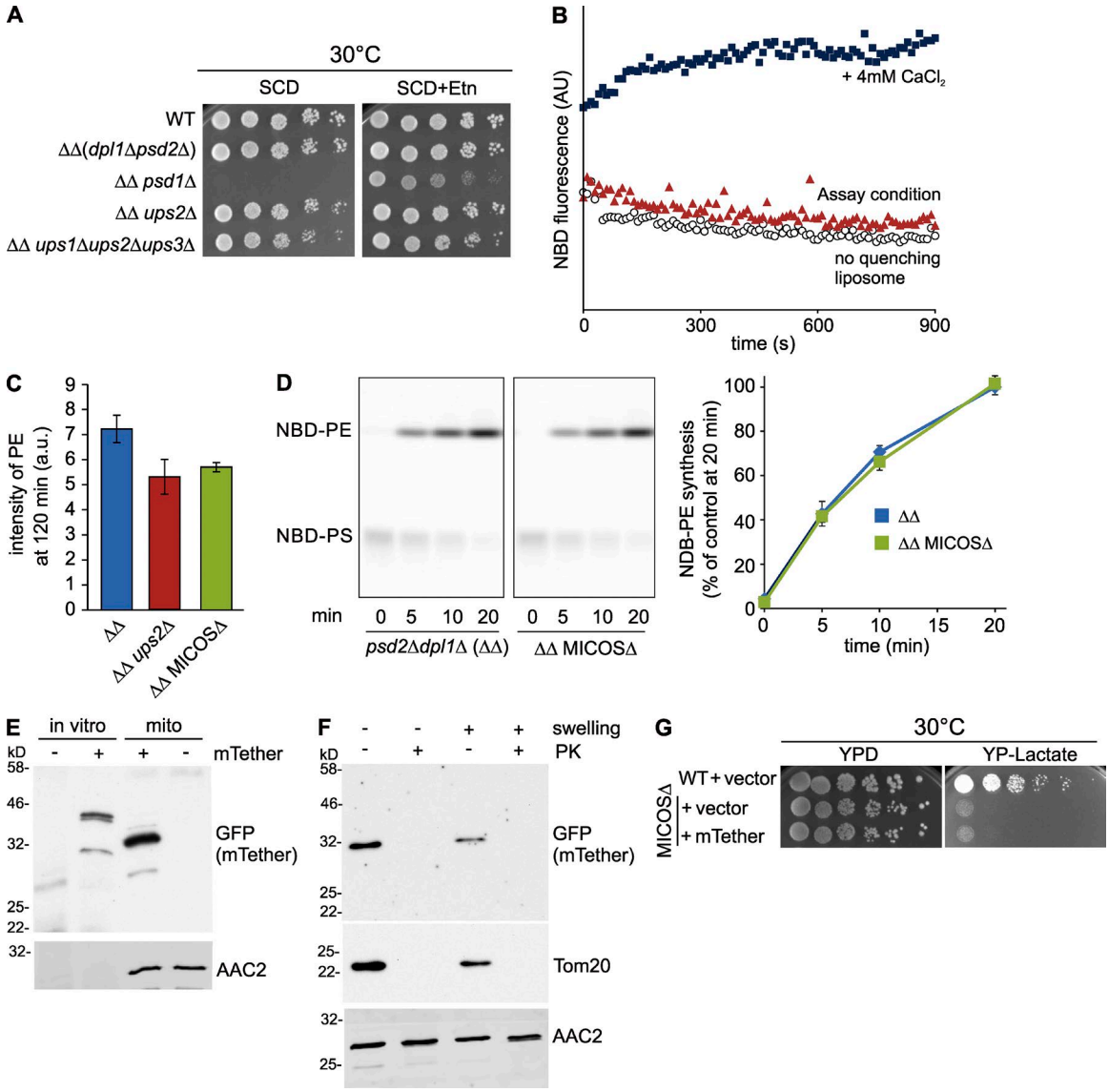

Figure S2. **Roles of membrane apposition and submitochondrial localization of the artificial membrane tether, related to Figs. 2 and 4.** (A) *dpl1*Δ *psd2*Δ*ups1*Δ*ups2*Δ*ups3*Δ cells did not show ethanolamine auxotrophy. Serial dilutions of the indicated cells were spotted on media with or without ethanolamine (Etn; 10 mM) and incubated at 30°C. Growth of *dpl1*Δ*psd2*Δ*psd1*Δ cells depended on ethanolamine. (B) Assessment of liposome fusion. Dequenching of NBD-PE in proteoliposomes upon dilution of quenching Rhodamine-PE by lipid mixing was monitored under identical conditions as the Psd1 activity assay (green triangles). Assay was performed in the absence of dequenching liposome K (open circles) or in the presence of fusogenic $CaCl_2$ (4 mM; blue square) as negative and positive controls. (C) Amount of labeled PE accumulating after a chase of 120 min after [^{14}C]serine labeling of cells vivo (corresponding to Figs. 2 B and 4 A). Error bars represent SEM. *n* = 3. (D) PS decarboxylase activity is not affected by the loss of MICOS. Isolated mitochondria (5 mg/ml) were incubated with soluble NBD-PS (16:0-6:0 NBD-PS, 2 µM) for indicated times at 30°C. Samples were mixed with chloroform/methanol (1:1) and subjected to lipid extraction and TLC analysis. Signals of PE were quantified and normalized to control cells (ΔΔ, mean value at 20 min). Error bars represent SEM. *n* = 3. (E) mTether accumulated in mitochondria is a processed form. Full-length precursor polypeptide of mTether was expressed in reticulocyte lysate and subjected to SDS-PAGE and immunodetection analysis together with samples of mitochondria isolated from cells expressing mTether. (F) Topology analysis of mTether. Isolated mitochondria from the *dpl1*Δ*psd2*ΔMICOSΔ cells expressing mTether were subjected to hypotonic swelling and/or protease treatment by proteinase K (50 µg/ml) as indicated. Samples were analyzed by SDS-PAGE and immunodetection using antibodies against indicated proteins. (G) Expression of mTether did not restore respiratory growth of MICOSΔ cells. Serial dilutions of indicated strains were spotted on YP medium containing glucose or lactate plate and incubated at 30°C.

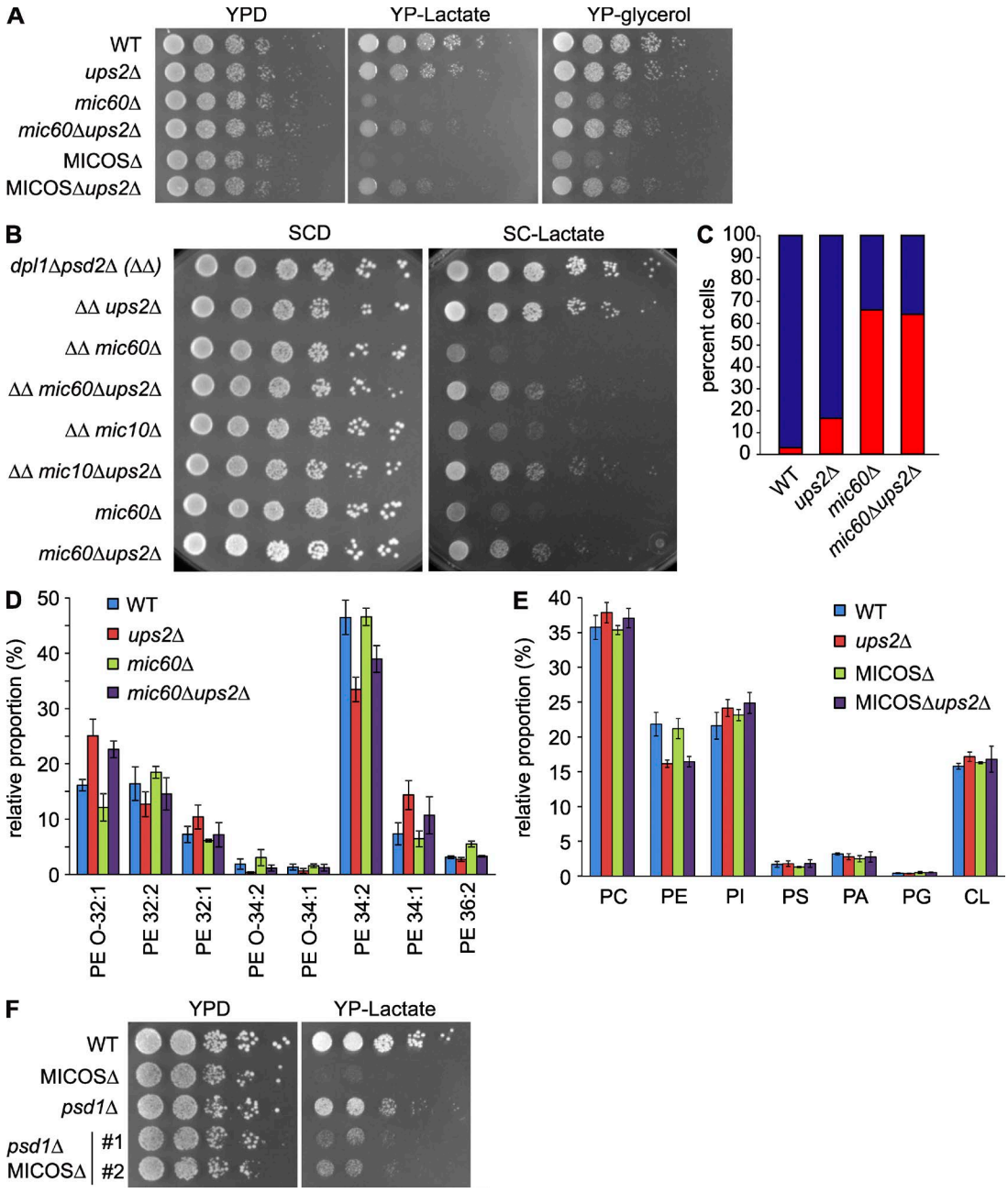

Figure S3. **Phenotypic consequences of the deletion of *UPS2* in cells lacking functional MICOS, related to Fig. 5.** (A) Deletion of *UPS2* restores respiratory growth of MICOSΔ cells. Serial dilutions of indicated strains (in W303 background) were spotted on YP medium containing glucose, glycerol, or lactate and incubated at 30°C. (B) Deletion of *UPS2* restores respiratory growth of cells lacking MICOS subunits in the absence of nonmitochondrial PE supply. Serial dilutions of indicated strains (in S288c background) were spotted on SC medium containing glucose (SCD) or lactate and incubated at 30°C. (C) Deletion of *UPS2* does not restore tubular mitochondria cells lacking Mic60. 200 cells of the indicated strains expressing mtGFP were analyzed by confocal microscopy and categorized into cells harboring tubular mitochondria (blue) and cells with fragmented or aggregated mitochondria (red). (D) Acyl-chain profile of mitochondrial PE determined by qMS. The indicated cells were grown on lactate medium (corresponding to Fig. 5 D). Error bars represent SEM. $n = 3$. (E) qMS of the mitochondrial phospholipidome in indicated strains grown in YP-lactate medium. Error bars represent SEM. $n = 3$. (F) Deletion of *PSD1* partially restored respiratory growth of MICOSΔ cells. Respiratory growth was assessed as in A.

Table S1. **Yeast strains used in the study**

Strain name	Strain description	Background	Genotype	Source
MA3	*dpl1Δpsd2Δmic60Δ*	S288c	*his3Δ1 leu2Δ0 (met15Δ0/MET15) lys2Δ0 ura3Δ0 mic60Δ::HisMX6*	This study
MA4	*dpl1Δpsd2Δups2Δmic60Δ*	S288c	*his3Δ1 leu2Δ0 (met15Δ0/MET15) lys2Δ0 ura3Δ0 ups2Δ::NatNT2 mic60Δ::HisMX6*	This study
MA27	*ups2Δmic60Δ*	S288c	*his3Δ1 leu2Δ0 (met15Δ0/MET15) lys2Δ0 ura3Δ0 ups2Δ::kanMX6 mic60Δ::KanMX6*	This study
MA28	*mic10Δ*	S288c	*his3Δ1 leu2Δ0 (met15Δ0/MET15) lys2Δ0 ura3Δ0 mic10Δ::HIS3*	This study
MA29	*dpl1Δpsd2Δmic10Δ*	S288c	*his3Δ1 leu2Δ0 (met15Δ0/MET15) lys2Δ0 ura3Δ0 mic10Δ::HisMX6*	This study
MA30	*dpl1Δpsd2Δ ups2Δmic10Δ*	S288c	*his3Δ1 leu2Δ0 (met15Δ0/MET15) lys2Δ0 ura3Δ0 ups2Δ::NatNT2 mic10Δ::HisMX6*	This study
MA43	*ups2Δmic10Δ*	S288c	*his3Δ1 leu2Δ0 (met15Δ0/MET15) lys2Δ0 ura3Δ0 ups2Δ::NatNT2 mic10Δ::HIS3*	This study
MA48	WT	W303	*ade2–1; leu2–3; his3–11, 15; trp1–1; ura3–1; can1–100*	Rothstein, 1983
MA49	*mic60Δ*	W303	*ade2–1; leu2–3; his3–11, 15; trp1–1; ura3–1; can1–100; mic60Δ::HIS3*	Friedman et al., 2015
MA50	*MICOSΔ*	W303	*ade2–1; leu2–3; his3–11, 15; trp1–1; ura3–1; can1–100; mic10Δ; mic60Δ; mic19Δ; mic27Δ; mic26Δ; mic12Δ*	Friedman et al., 2015
MA51	*ups2Δ*	W303	*ade2–1; leu2–3; his3–11, 15; trp1–1; ura3–1; can1–100; ups2Δ::NatNT2*	This study
MA53	*mic60Δups2Δ*	W303	*ade2–1; leu2–3; his3–11, 15; trp1–1; ura3–1; can1–100; mic60Δ::HIS3; ups2Δ::NatNT2*	This study
MA55	*MICOSΔups2Δ*	W303	*ade2–1; leu2–3; his3–11, 15; trp1–1; ura3–1; can1–100; mic10Δ; mic60Δ; mic19Δ; mic27Δ; mic26Δ; mic12Δ ups2Δ::NatNT2*	This study
MA82	*psd1Δ*	W303	*ade2–1; leu2–3; his3–11, 15; trp1–1; ura3–1; can1–100; psd1Δ::KanMX6*	This study
MA85	*psd1ΔMICOSΔ*	W303	*ade2–1; leu2–3; his3–11, 15; trp1–1; ura3–1; can1–100; mic10Δ; mic60Δ; mic19Δ; mic27Δ; mic26Δ; mic12Δ; psd1Δ::KanMX6*	This study
MA86	*psd1ΔMICOSΔ #2*	W303	*ade2–1; leu2–3; his3–11, 15; trp1–1; ura3–1; can1–100; mic10Δ; mic60Δ; mic19Δ; mic27Δ; mic26Δ; mic12Δ psd1Δ::KanMX6*	This study
MA97	*dpl1Δpsd2Δ*	W303	*ade2–1; leu2–3; his3–11, 15; trp1–1; ura3–1; can1–100; dpl1Δ::hphNT1; psd2Δ::KanMX6*	This study
MA 101	*dpl1Δpsd2 ΔMICOSΔ*	W303	*ade2–1; leu2–3; his3–11, 15; trp1–1; ura3–1; can1–100; dpl1Δ::hphNT1; psd2Δ::KanMX6; mic10Δ; mic60Δ; mic19Δ; mic27Δ; mic26Δ; mic12Δ*	This study
MA103	*dpl1Δpsd2Δups2Δ*	W303	*ade2–1; leu2–3; his3–11, 15; trp1–1; ura3–1; can1–100; dpl1Δ::hphNT1; psd2Δ::KanMX6; ups2Δ::NatNT2*	This study
MA107	*ups2ΔMICOSΔ*	W303	*ade2–1; leu2–3; his3–11, 15; trp1–1; ura3–1; can1–100; mic10Δ; mic60Δ; mic19Δ; mic27Δ; mic26Δ; mic12Δ ups2Δ::NatNT2*	This study
MA170	*ups1Δups2Δups3Δ dpl1Δpsd2Δ*	W303	*ade2–1; leu2–3; his3–11, 15; trp1–1; ura3–1; can1–100; ups3Δ::URA3; ups1Δ::HIS3; dpl1Δ::hphNT1; psd2Δ::KanMX6; ups2Δ::NatNT2*	This study
MA233	*psd1Δdpl1Δpsd2Δ*	W303	*ade2–1; leu2–3; his3–11, 15; trp1–1; ura3–1; can1–100; psd1Δ::HIS3; dpl1Δ::hphNT1; psd2Δ::KanMX6*	This study
MC68	*mic60Δ*	S288c	*his3Δ1 leu2Δ0 (met15Δ0/MET15) lys2Δ0 ura3Δ0 mic60Δ::KanMX6*	This study
CG214	Wild-type	S288c	*his3Δ1leu2Δ0 met15Δ0 lys2Δ0 ura3Δ0*	Osman et al., 2009
CG232	*ups2Δ*	S288c	*his3Δ1 leu2Δ0 (met15Δ0/MET15; lys2Δ0/LYS2) ura3Δ0 ups2Δ::NatNT2*	Osman et al., 2009
CG547	*ups2Δphb1Δ +pCM189-PHB1 +Yeplac181*	S288c	*his3Δ1 leu2Δ0 (met15Δ0/MET15; lys2Δ0/LYS2) ura3Δ0 ups2Δ::KanMX6 phb1Δ::NatNT2 pCM189-PHB1 +Yeplac181*	Osman et al., 2009
CG548	*ups2Δphb1Δ +pCM189-PHB1 +pYX142-PHB1*	S288c	*his3Δ1 leu2Δ0 (met15Δ0/MET15; lys2Δ0/LYS2) ura3Δ0 ups2Δ::kanMX6 phb1Δ::NatNT2 +pCM189-PHB1 +pYX142-PHB1*	Osman et al., 2009
CG585	*dpl1Δpsd2Δ*	S288c	*ade2–1; leu2–3; his3–11, 15; trp1–1; ura3–1; can1–100; dpl1Δ::hphNT1; psd2Δ::KanMX6*	This study
CG586	*dpl1Δpsd2Δ Δups2*	S288c	*ade2–1; leu2–3; his3–11, 15; trp1–1; ura3–1; can1–100; dpl1Δ::hphNT1; psd2Δ::KanMX6; ups2Δ::NatNT2*	This study

References

Friedman, J.R., A. Mourier, J. Yamada, J.M. McCaffery, and J. Nunnari. 2015. MICOS coordinates with respiratory complexes and lipids to establish mitochondrial inner membrane architecture. *eLife.* 4. http://dx.doi.org/10.7554/eLife.07739

Osman, C., M. Haag, C. Potting, J. Rodenfels, P.V. Dip, F.T. Wieland, B. Brügger, B. Westermann, and T. Langer. 2009. The genetic interactome of prohibitins: Coordinated control of cardiolipin and phosphatidylethanolamine by conserved regulators in mitochondria. *J. Cell Biol.* 184:583–596. http://dx.doi.org/10.1083/jcb.200810189

Rothstein, R.J. 1983. One-step gene disruption in yeast. *Methods Enzymol.* 101:202–211. http://dx.doi.org/10.1016/0076-6879(83)01015-0